arXiv:astro-ph/9909020v1 1 Sep 1999

Dust sublimation by GRBs and its implications

E. Waxman[1] and B. T. Draine[2]
[1]Department of Condensed-Matter Physics, Weizmann Institute, Rehovot 76100, Israel
[2]Princeton University Observatory, Peyton Hall, Princeton, NJ 08544

ABSTRACT

The prompt optical flash recently detected accompanying GRB990123 suggests that, for at least some GRBs, γ-ray emission is accompanied by prompt optical-UV emission with luminosity $L(1-7.5\,\mathrm{eV}) \approx 1\times10^{49}(\Delta\Omega/4\pi)\mathrm{erg/s}$, where $\Delta\Omega$ is the solid angle into which γ-ray and optical-UV emission is beamed. Such an optical-UV flash can destroy dust *in the beam* by sublimation out to an appreciable distance, ≈ 10 pc, and may clear the dust out of as much as $\sim 10^7(\Delta\Omega/4\pi)M_\odot$ of molecular cloud material on an apparent time scale of $\sim$ ten seconds. Detection of time dependent extinction on this time scale would therefore provide strong constraints on the GRB source environment. Dust destruction implies that existing, or future, observations of not-heavily-reddened fireballs are not inconsistent with GRBs being associated with star forming regions. In this case, however, if γ-ray emission is highly beamed, the expanding fireball would become reddened on a $\sim$1 week time scale.

If the optical depth due to dust beyond ≈ 8 pc from the GRB is $0.2 \lesssim \tau_V \lesssim 2$, most of the UV flash energy is converted to infra-red, $\lambda \approx 1\mu$m, radiation with luminosity $L_{\mathrm{IR}} \approx 10^{41}$erg/s extending over an apparent duration of $\approx 20(1+z)(\Delta\Omega/0.01)$ day. Dust infra-red emission may already have been observed in GRB970228 and GRB980326, and may possibly explain their unusual late time behavior.

Subject headings: Gamma Rays: Bursts– ISM: Dust, Extinction

1. Introduction

A prompt, 9-th magnitude, optical flash has recently been detected (Akerlof *et al.* 1999) accompanying the gamma ray burst (GRB) GRB990123. The most natural explanation of this flash is emission from a reverse shock propagating into fireball ejecta shortly after it interacts with surrounding gas (Sari & Piran 1999b, Mészáros & Rees 1999). Although optical-UV emission from the reverse shock accompanying, or following shortly after, the γ-ray emission has been predicted (Mészáros, Rees & Papathanassiou 1994, Mészáros & Rees 1997, Panaitescu & Mészáros 1998, Sari & Piran 1999a) based on the simplest fireball models for gamma-ray bursts (GRBs), the intensity of optical emission could not have been reliably predicted due to the uncertainty in reverse shock parameters. The observations of GRB990123 suggest that the electron and magnetic

field energy fractions in the reverse shock are similar to those in the forward shock propagating into the surrounding gas and producing the long term afterglow. This in turn implies that strong optical flashes accompanying γ-ray emission is a generic GRB characteristic. This is consistent with previous non-detection of optical flashes (Park *et al.* 1997) given the wide GRB luminosity function (Krumholtz, Thorsett & Harrison 1998, Mau & Mo 1998, Hogg & Fruchter 1998) and the fact that GRB990123 is in the top 0.3% of the BATSE brightness distribution (Kouveliotou *et al.* 1999).

There is evidence in several GRB afterglows for significant dust extinction, which may imply an association of GRBs with star forming regions (Kulkarni *et al.* 1998, Metzger *et al.* 1997, Paczyński 1998). It has been shown that if GRBs indeed reside in such environment, the ionizing X-ray and UV afterglow radiation may lead to time dependent (on hour time scale) absorption (Perna & Loeb 1998) and emission (Ghisellini *et al.* 1998, Böttcher *et al.* 1998) line features. If H_2 is present near the GRB, conspicuous 1110–1650Åabsorption will be imprinted on the spectrum, followed by UV fluorescence (Draine 1999b). On longer time scales, up to $\sim 10^5$ yr, GRB photo-ionization may lead to indicative recombination line features, which may allow identification of GRB remnants in nearby galaxies (Loeb & Perna 1998, Perna, Raymond & Loeb 1999). Here, we discuss dust sublimation by the optical-UV flash accompanying the GRB. Since GRB990123 was an exceptionally bright burst, with exceptionally high intrinsic γ-ray luminosity, we first discuss in §2 the optical-UV flash itself to obtain the scaling of optical-UV luminosity with burst energy, and to estimate the prompt optical-UV emission at energies above the $2(1+z)$ eV energy of the prompt emission observed by Akerlof et al. We show that if electron and magnetic field energy fractions in the reverse shock are similar among different bursts, then an optical-UV flash of luminosity $L_{\rm UV} \approx 3\times10^{49}(\Delta\Omega/4\pi)$erg/s, where $\Delta\Omega$ is the beaming solid angle, is expected for a typical GRB. Dust destruction by thermal sublimation is discussed in §3, and other possible destruction mechanism are considered in §4. It should be emphasized that the analysis of the physics of dust destruction is independent of the model for optical-UV emission, and therefore of the discussion presented in §2. However, we present numerical results for dust destruction based on the characteristic optical-UV luminosity derived in §2. In §5 we discuss dust infra-red emission. The implications of our results are discussed in §6.

2. The Prompt Optical-UV Luminosity

2.1. Fireball Dynamics

In fireball models of GRBs (see Piran 1998 for a recent review), the energy released by an explosion is converted to kinetic energy of a thin baryonic shell expanding at an ultra-relativistic speed. After producing the GRB, the shell impacts on surrounding gas, driving an ultra-relativistic shock into the ambient medium. After a short transition phase, the expanding blast wave approaches a self-similar behavior (Blandford & McKee 1976), where the expansion Lorentz factor

decreases with radius as $\Gamma \propto r^{-3/2}$. The initial interaction of fireball ejecta with surrounding gas produces a reverse shock which propagates into and decelerates the fireball ejecta. Transition to self-similar behavior occurs on a time scale comparable to the reverse shock crossing time of the ejecta.

The long term afterglow is produced by the forward, expanding shock that propagates into the surrounding gas. This shock continuously heats fresh gas and accelerates relativistic electrons, which produce the observed radiation through synchrotron emission. The most natural explanation of the optical flash is that it is due to synchrotron emission of electrons which are accelerated by the reverse shock, during the transition to self-similar behavior. Once the reverse shock crosses the ejecta, the ejecta expand and cool adiabatically. Thus, emission from the fireball ejecta is suppressed after the transition to self-similar expansion.

Since the optical flash is produced when the reverse shock crosses the ejecta, the plasma emitting the radiation expands with a Lorentz factor which is close to that given by the Blandford-McKee self-similar solution, $\Gamma = (17E/16\pi n m_p c^2)^{1/2} r^{-3/2}$, where E is the fireball energy and n is the surrounding gas number density. The characteristic time over which radiation emitted by the fireball at radius r is observed by a distant observer is $\Delta t \approx r/4\Gamma^2 c$ (Waxman 1997c). The plasma Lorentz factor during optical flash emission

$$\Gamma \simeq \left(\frac{17E}{1024\pi n m_p c^5}\right)^{1/8} \left(\frac{\Delta t^{\rm ob.}}{1+z}\right)^{-3/8} = 345 \left(\frac{E_{53}}{n_0}\right)^{1/8} \left(\frac{2.5}{1+z}\Delta t_1^{\rm ob.}\right)^{-3/8}, \tag{1}$$

where $E = 10^{53} E_{53}$ erg, $\Delta t^{\rm ob.} = 10 \Delta t_1^{\rm ob.}$ s is the observed duration, $\Delta t^{\rm ob.} = (1+z)\Delta t$, and $n = 1 n_0 \,{\rm cm}^{-3}$.

Transition to self-similar expansion occurs on time scale $\Delta t^{\rm ob.}$ comparable to the longer of the two time scales set by the initial conditions: the (observed) GRB duration $\Delta t_{\rm GRB}$ and the (observed) time Δt_Γ at which the self-similar Lorentz factor equals the original ejecta Lorentz factor Γ_i, $\Gamma(\Delta t^{\rm ob.} = \Delta t_\Gamma) = \Gamma_i$. That is,

$$\Delta t^{\rm ob.} = \max\left[\Delta t_{\rm GRB}, 15\frac{1+z}{2.5}\left(\frac{E_{53}}{n_0}\right)^{1/3}\left(\frac{\Gamma_i}{300}\right)^{-8/3} {\rm s}\right]. \tag{2}$$

During the transition, the unshocked fireball ejecta propagate at the original expansion Lorentz factor, $\Gamma_i > \Gamma$, and the Lorentz factor of plasma shocked by the reverse shock in the rest frame of the unshocked ejecta is $\simeq \Gamma_i/\Gamma$. If $\Delta t^{\rm ob.} \simeq \Delta t_{\rm GRB} \gg \Delta t_\Gamma$ then $\Gamma_i/\Gamma \gg 1$, the reverse shock is relativistic, and the Lorentz factor associated with the random motion of protons in the reverse shock is $\gamma_p^R \simeq \Gamma_i/\Gamma$. If $\Delta t^{\rm ob.} \simeq \Delta t_\Gamma \gg \Delta t_{\rm GRB}$ then $\Gamma_i/\Gamma \sim 1$, and the reverse shock is not relativistic. Nevertheless, the following argument suggests that the reverse shock speed is not far below c, and that the protons are therefore heated to relativistic energy, $\gamma_p^R - 1 \simeq 1$. The comoving time, measured in the fireball ejecta frame prior to deceleration, is $t_{\rm co.} \simeq r/\Gamma_i c$. The expansion Lorentz factor is expected to vary across the ejecta, $\Delta\Gamma_i/\Gamma_i \sim 1$. Such variation would lead to expansion of the ejecta, in the comoving frame, at relativistic speed. Thus, at the deceleration

radius, $t_{\rm co.} \simeq \Gamma_i \Delta t$, the ejecta width exceeds $\simeq ct_{\rm co.} \simeq \Gamma_i c\Delta t$. Since the reverse shock should cross the ejecta over a deceleration time scale, $\simeq \Gamma\Delta t$, the reverse shock speed must be close to c. We therefore conclude that the Lorentz factor associated with the random motion of protons in the reverse shock is approximately given by $\gamma_p^R - 1 \simeq \Gamma_i/\Gamma$ for both $\Gamma_i/\Gamma \sim 1$ and $\Gamma_i/\Gamma \gg 1$. For protons shocked by the forward shock $\gamma_p^F \simeq \Gamma$, and therefore the ratio between thermal energy per proton in the reverse and forward shocks is $(\gamma_p^R - 1)/(\gamma_p^F - 1) \simeq \Gamma_i/\Gamma^2$. Below we use this relation to derive the emission characteristics of the reverse shock by scaling the exact analytic results given for the forward shock emission in Gruzinov & Waxman (1999).

2.2. Optical-UV Emission

If the fraction of thermal energy carried by electrons, ξ_e, and magnetic field, ξ_B, is similar in the forward and reverse shocks, then the frequency of peak synchrotron emission from the reverse shock is smaller than that of the forward shock by a factor $\simeq (\Gamma_i/\Gamma^2)^2$. This is due to the fact that the energy density behind the reverse and forward shocks are similar, so that similar ξ_B implies similar magnetic field strength in both regions, while similar ξ_e implies $\gamma_e^R/\gamma_e^F \simeq (\gamma_p^R - 1)/(\gamma_p^F - 1) \simeq \Gamma_i/\Gamma^2$. Using Eq. (10) of Gruzinov & Waxman (1999) for the forward shock peak frequency, we find that the reverse shock emission peaks at a frequency

$$\nu_m \approx 1.7 \times 10^{14} \left(\frac{\xi_e}{0.2}\right)^2 \left(\frac{\xi_B}{0.01}\right)^{1/2} \left(\frac{\Gamma_i}{300}\right)^2 n_0^{1/2} {\rm Hz} \tag{3}$$

(measured at the GRB redshift). Here ξ_e and ξ_B are the values relevant for the reverse shock, which in general may differ from those of the forward shock. The numerical values we have used are those characteristic of the forward shock (Waxman 1997a, Waxman 1997b, Wijers & Galama 1998, Granot *et al.* 1998).

As demonstrated below, the cooling time of electrons in the reverse shock, radiating in the optical-UV range, is long compared to the fireball expansion time. In this case, the peak synchrotron intensity is proportional to the product of magnetic field strength and number of radiating electrons (and independent of the electron Lorentz factor). The number of radiating electrons in the reverse shock is larger than in the forward shock by a factor Γ^2/Γ_i. This can be deduced from the following considerations. The proton random Lorentz factor in the reverse shock is Γ^2/Γ_i times smaller than that in the forward shock. Since the energy density in both regions is similar, the density of protons, and therefore of electrons, in the reverse shock is higher than that in the forward shock by the same factor. In addition, the width of the shocked fireball ejecta is similar to that of the shell of shocked surrounding gas, since both shocks propagate relativistically in the shocked plasma frame. Thus, if ξ_B is similar in the reverse and forward shock, the peak synchrotron intensity f_m is higher in the reverse shock by a factor Γ^2/Γ_i. Using Eq. (11) of

Gruzinov & Waxman (1999) we find for the reverse shock

$$f_m \approx 1h_{65}^2 \left(\frac{\sqrt{2.5}-1}{\sqrt{1+z}-1}\right)^2 \left(\frac{\xi_B}{0.01}\right)^{1/2} \left(\frac{\Gamma_i}{300}\right)^{-1} n_0^{1/4} E_{53}^{5/4} \left(\frac{2.5}{1+z}\Delta t_1^{\rm ob.}\right)^{-3/4} \ {\rm Jy} \tag{4}$$

for a flat universe with zero cosmological constant, and $H_0 = 65h_{65}$km/s Mpc.

The decay of GRB990123 optical flux implies an electron energy distribution $dN_e/dE_e \propto E_e^{-p}$ with $p \approx 2$ (Mészáros & Rees 1999), for which the intensity at $\nu > \nu_m$ is $f_\nu \propto \nu^{-1/2}$. Thus, the optical [$\nu = (5(1+z) \times 10^{14}$ Hz] intensity is

$$f_V \approx 0.4h_{65}^2 \left(\frac{2.5}{1+z}\right)^{1/2} \left(\frac{\sqrt{2.5}-1}{\sqrt{1+z}-1}\right)^2 \left(\frac{\xi_e}{0.2}\right) \left(\frac{\xi_B}{0.01}\right)^{3/4} n_0^{1/2} E_{53}^{5/4} \left(\frac{2.5}{1+z}\Delta t_1^{\rm ob.}\right)^{-3/4} \ {\rm Jy}. \tag{5}$$

For the parameters of GRB990123, $\Delta t^{\rm ob.} \approx 60$ s and $E \approx 10^{54}$ erg (based on the γ-ray fluence $\sim 3 \times 10^{-4}{\rm erg\,cm^{-2}}$), we obtain $f_V \approx 2$ Jy, approximately twice the peak observed flux. Thus, the observed optical flash can be naturally explained by the simplest fireball model, provided the reverse shock parameters ξ_e and ξ_B are similar to those implied for the forward shock by afterglow observations, $\xi_e \approx 0.2$ and $\xi_B \approx 0.01$. If this is typical, than for a typical GRB, with $E \sim 10^{53}$ erg and $\Delta t^{\rm ob.} \approx 10$ s, we find

$$L_\nu = \frac{4\pi d_L^2}{1+z} f_\nu \approx 10^{34} \left(\frac{\xi_e}{0.2}\right) \left(\frac{\xi_B}{0.01}\right)^{3/4} n_0^{1/2} E_{53}^{5/4} \left(\frac{2.5}{1+z}\Delta t_1^{\rm ob.}\right)^{-3/4} \left(\frac{\nu}{10^{15}{\rm Hz}}\right)^{-1/2} \ {\rm erg/s\ Hz}. \tag{6}$$

where ν is the frequency at the redshift of the GRB. The form (6) is valid for frequencies ν larger than the peak frequency ν_m, and smaller than the frequency ν_c above which emission is dominated by electrons for which the cooling time is shorter than the dynamic time. Since the energy density in the reverse and forward shock regions is similar, ν_c (at the GRB redshift) is given by

$$\nu_c \sim 10^{17} \left(\frac{\xi_B}{0.01}\right)^{-3/2} n_0^{-1} E_{53}^{-1/2} \left(\frac{2.5}{1+z}\Delta t_1^{\rm ob.}\right)^{-1/2} \ {\rm Hz}. \tag{7}$$

At frequencies $\nu > \nu_c$ the spectrum steepens to $L_\nu \propto \nu^{-1}$.

Strong optical-UV emission requires, similar to GRB γ-ray production, large initial Lorentz factor, $\Gamma_i > 100$: Eq. (2) implies that $\Delta t \propto \Gamma_i^{-8/3}$ for $\Gamma_i \lesssim 300$, and the optical-UV luminosity given by Eq. (6) drops as $L_\nu \propto \Gamma_i^2$. This implies that the plasma emitting the optical-UV photons must also be expanding at high Lorentz factor, $\Gamma > 100$ [see Eqs. (2,1)], and strong optical-UV emission may be confined, similar to γ-rays, to a cone around the line of sight of opening angle $1 \gg \theta_\gamma > 1/\Gamma \sim 0.01$. This may be the case if, e.g., the fireball is a jet of opening angle $\theta_j = \theta_\gamma$. A jet of finite opening angle expands as if it were a conical section of a spherical fireball, as long as $\theta_j > 1/\Gamma$. Thus, the analysis presented above is valid for a jet-like fireball. In this case, the energy E in the above equations should be understood as the energy that the fireball would have carried if it were spherically symmetric, and the optical-UV, as well as γ-ray, emission is confined to a small solid angle $\Delta\Omega = \pi\theta_j^2$ with optical-UV luminosity given by $\Delta\Omega L_\nu$.

It should be noted that prompt optical emission has been observed for only 1 GRB to date, and therefore may not be typical of GRBs. Indeed, fireballs in low density environments with $n \ll 1\,\mathrm{cm}^{-3}$ would not be expected to produce strong prompt emission [see Eq. (5)]. However, we note from Eq. (5) that optical flashes are expected for typical GRBs with $E_{53} \approx 1$ and $n_0 \gtrsim 1$, and should not be limited to unusually luminous GRBs such as GRB990123.

3. Dust Destruction by Thermal Sublimation

As discussed in §3.3 below, in dense regions radiation with $h\nu > 13.6$ eV will largely go into photoionizing H and H_2, and photons in the 7.5–13.6 eV range will primarily be absorbed by H_2, which is rovibrationally excited by ultraviolet pumping (Draine 1999b). We therefore first discuss, in §3.1 and §3.2, sublimation of dust grains under the assumption that dust heating is dominated by $1\,\mathrm{eV} < h\nu < 7.5$ eV photons, and discuss the contribution of 7.5–50 eV photons to dust sublimation in §3.3. Using equations (6) and (7), we find that for typical GRB parameters, the prompt luminosity in the 1–7.5 eV range is 2×10^{49} erg/s and the 7.5–50 eV prompt luminosity is $\sim 5 \times 10^{49}$ erg/s. Since our simple analysis overestimates the flux of GRB990123 by a factor ~ 2, we will take the typical 1–7.5 eV luminosity to be $L_{1-7.5} = 10^{49} L_{49}$erg/s, and the 7.5–50 eV luminosity to be $L_{7.5-50} = 2.5 \times 10^{49} L_{49}$ erg/s.

3.1. Grain Heating

Consider a grain of radius a located at a distance r from a transient source of radiation radiating a 1–7.5 eV power $L_{1-7.5}(\Delta\Omega/4\pi)$ into a solid angle $\Delta\Omega$. If the radiation from the GRB is "beamed" into $\Delta\Omega < 4\pi$, we will consider only dust grains within the beam. Note that we expect the beaming of optical-UV emission from the forward shock to be similar to that of gamma-ray emission.

The grain temperature T is determined by

$$e^{-\tau} \frac{L_{1-7.5}}{4\pi r^2} Q_{\mathrm{UV}} \pi a^2 = \langle Q \rangle_T 4\pi a^2 \sigma T^4 - 4\pi a^2 \frac{da}{dt} \frac{\rho}{m} B \quad , \tag{8}$$

where τ is the effective optical depth for attenuation of the optical-UV flash, ρ is the density of the grain material, m is the mean atomic mass, B is the chemical binding energy per atom,

$$\langle Q \rangle_T \equiv \frac{\int B_\nu(T) Q_{\mathrm{abs},\nu} d\nu}{\int B_\nu(T) d\nu} \tag{9}$$

is the usual Planck-averaged absorption efficiency, and Q_{UV} is the absorption efficiency factor averaged over the 1–7.5 eV spectrum of the optical-UV flash. For the grain radii $a \gtrsim 10^{-5}\,\mathrm{cm}$ expected in dense clouds, we will assume $Q_{\mathrm{UV}} \approx 1$. Since we are interested in energy depositions large enough to sublime grains, the heat capacity of the grain has been neglected in equation (8).

The sublimation rate can be approximated by

$$\frac{da}{dt} = -\left(\frac{m}{\rho}\right)^{1/3} \nu_0 e^{-B/kT} \ . \tag{10}$$

Guhathakurta & Draine (1989) have estimated $\nu_0 \approx 2 \times 10^{15}\mathrm{s}^{-1}$, $B/k = 68100\mathrm{K}$ for Mg_2SiO_4, and $\nu_0 = 2 \times 10^{14}\mathrm{s}^{-1}$, $B/k = 81200\mathrm{K}$ for graphite. We adopt $\nu_0 = 1 \times 10^{15}\mathrm{s}^{-1}$, $B/k = 7 \times 10^4\mathrm{K}$, and $\rho/m \approx 10^{23}\,\mathrm{cm}^{-3}$ as representative values for refractory grains. If we assume the grain temperature T is approximately constant over the time $\Delta t = \Delta t^{\mathrm{ob.}}/(1+z)$, then the condition for the grain to be completely sublimed during this time would be $T > T_c$, where

$$T_c = \frac{B/k}{\ln\left[(m/\rho)^{1/3}\left(\nu_0 \Delta t/a\right)\right]} \approx 2300\mathrm{K}\left[1 + 0.033\ln\left(\frac{a_{-5}}{\Delta t_1}\right)\right] \tag{11}$$

where $a_{-5} \equiv a/10^{-5}\,\mathrm{cm}$. Equivalently, the grain survival time at temperature T is

$$t_{\mathrm{surv}}(T) = \frac{a}{|da/dt|} = 7.7 a_{-5} \exp\left[7 \times 10^4\,\mathrm{K}\left(\frac{1}{T} - \frac{1}{2300\,\mathrm{K}}\right)\right]\ \mathrm{s} \quad . \tag{12}$$

The infrared emissivity is quite different for graphite and silicate materials (Draine & Lee 1984; Draine 1999a). For the temperature range of interest for dust sublimation, $2000\,\mathrm{K} \lesssim T \lesssim 3000\,\mathrm{K}$, we approximate

$$\langle Q \rangle_T \approx \frac{A a_{-5}(T/2300\mathrm{K})}{1 + A a_{-5}(T/2300\mathrm{K})} \tag{13}$$

with $A \approx 0.03$ and 0.3 for astronomical silicate and graphite, respectively. We adopt equation (13) with $A = 0.1$ as representative of refractory grain material.

Radiation and sublimation then contribute equally to the cooling at a temperature $T_{\mathrm{r=s}}$ determined by

$$T_{\mathrm{r=s}} = 2820\,\mathrm{K}\left\{1 - 0.040\ln\left[\left(\frac{T_{\mathrm{r=s}}}{2800\,\mathrm{K}}\right)^4 \frac{a_{-5}(T_{\mathrm{r=s}}/2300\,\mathrm{K})}{1 + 0.1 a_{-5}(T_{\mathrm{r=s}}/2300\,\mathrm{K})}\right]\right\}^{-1} \quad . \tag{14}$$

For $T > T_{\mathrm{r=s}}$, so that sublimation cooling dominates over radiative cooling, the grain temperature is

$$T_{\mathrm{sub}} \approx 3030\mathrm{K}\left[1 + 0.043\ln(Q_{\mathrm{UV}} e^{-\tau} L_{49} r_{19}^{-2})\right] \quad , \tag{15}$$

where $r \equiv 10^{19} r_{19}\,\mathrm{cm}$.

For $T < T_{\mathrm{r=s}}$ radiative cooling dominates and the grain temperature is

$$T_{\mathrm{rad}} = \left(e^{-\tau}\frac{L_{1-7.5}}{16\pi\sigma r^2}\frac{Q_{\mathrm{UV}}}{\langle Q \rangle_T}\right)^{1/4} = 2160\mathrm{K}\left(e^{-\tau}\frac{L_{49} Q_{\mathrm{UV}}}{\langle Q \rangle_T/0.1}\right)^{1/4}\left(\frac{r_{19}}{4}\right)^{-1/2} \quad . \tag{16}$$

where $e^{-\tau}$ is the instantaneous attenuation of the 1–7.5 eV flash by intervening absorption.

If attenuation by intervening material can be neglected, grains are completely sublimed out to a destruction radius $R_{\rm d} = R_{\rm c}$ where $R_{\rm c}$ is the radius where the unattenuated flash can heat grains to the critical temperature T_c. For our nominal parameters, Eq. (11) and (14) give $T_c < T_{r=s}$, so that radiative cooling dominates at $r = R_{\rm c}$, and the critical distance $R_{\rm c}$ is given by

$$R_{\rm c} = \left(\frac{L_{1-7.5}}{16\pi\sigma T_c^4}\frac{Q_{\rm UV}}{\langle Q\rangle_{T_c}}\right)^{1/2} \approx 3.7\times 10^{19}\left(\frac{Q_{\rm UV}L_{49}(1+0.1a_{-5})}{a_{-5}}\right)^{1/2}\ {\rm cm} \quad . \tag{17}$$

In the optically-thin limit, then, the optical-UV flash from the GRB will destroy dust *in the beam* out to a substantial distance.

3.2. Effects of Dust Optical Depth

While the 1–7.5 eV photons from a GRB may be capable of destroying dust out to $R_{\rm c} \approx 10$ pc in the optically-thin limit, in dusty regions (such as molecular clouds) attenuation of the radiation by dust grains before they are destroyed will limit the grain destruction to a smaller radius. The dust optical depth is a function $\tau(r,t)$ of both space and time, as the GRB flash "burns" its way through the cloud.

The attenuation of $\sim$1–7.5 eV photons is dominated by dust. To estimate the effect of high optical depth, we will assume that only a single dust type is present. Let $R_{\rm d}$ be the dust destruction radius: all grains at $r < R_{\rm d}$ are destroyed by the heating effects of the optical-UV flash.

We approximate the 1–7.5 eV emission from the GRB as a rectangular pulse. At radii $r < R_{\rm d}$, the *leading* edge of the optical-UV pulse is attenuated by the dusty medium through which it propagates, but the *trailing* edge of the pulse is unattenuated since it propagates through a dustless medium, and we are neglecting the effects of gas-phase absorption. Rather than solve for $\tau(r,t)$, we will simplify the problem by assuming that the effects of extinction can be approximated as primarily a *narrowing* of the optical pulse, retaining a rectangular profile. The problem then reduces to determination of a function $f(r)$, the fraction of the flash energy which is absorbed by dust interior to radius r, and survival of grains at radius r when irradiated by a radiation field $L_{1-7.5}/4\pi r^2$ for a time $(1-f)\Delta t$.

The function $f(r)$ then satisfies

$$\frac{df}{dr} = Q_{\rm UV} n_d \pi a^2 \frac{\min[t_{\rm surv},(1-f)\Delta t]}{\Delta t} \tag{18}$$

where $t_{\rm surv}(r)$ is the survival time of a grain irradiated by the unattenuated radiation field. In the unattenuated portion of the optical pulse, grains are heated to temperatures given by equations (15,16) with $\tau = 0$. The dust destruction radius $R_{\rm d}$ is then determined by the condition $t_{\rm surv}(T(R_{\rm d})) = [1 - f(R_{\rm d})]\Delta t$.

Figure 1 shows $R_{\rm d}$ as a function of cloud density $n_{\rm H} = n({\rm H}) + 2n({\rm H}_2)$ for a standard dust-to-gas ratio $n_d(4\pi/3)a^3\rho/n_{\rm H}m_{\rm H} = 0.01$, for several different values of the GRB 1–7.5 eV luminosity (L_{49}), duration (Δt_1), and characteristic dust grain radius (a_{-5}). The radius R_d for "typical" GRB parameters is shown as the heavy curve. We see that if a GRB occurred in a dusty region, the optical-UV flash from the GRB can clear out a substantial amount of dust which lies in the beam.

3.3. H and H_2 Absorption

Radiation with $h\nu > 13.6$ eV may ionize H and H_2. Neglecting dust opacity, the prompt flash will be able to photoionize a mass

$$M_{\rm ion} \approx \frac{m_{\rm H}L_{13.6-50}\Delta t}{25\,{\rm eV}} \approx 4\times10^3 M_\odot L_{49}\Delta t_1 \tag{19}$$

or out to a radius

$$R_{\rm ion} \approx 1.2\times10^{19}\,{\rm cm}\left(\frac{L_{49}\Delta t_1}{n_3}\right)^{1/3} \tag{20}$$

where $n_3 \equiv n_{\rm H}/10^3\,{\rm cm}^{-3}$, and we approximate the flash by a rectangular pulse of duration $\Delta t = 10\Delta t_1$ s. We have taken the typical 13.6–50 eV luminosity to be $\sim 2\times10^{49}L_{49}\,{\rm ergs\,s}^{-1}$.

The dust destruction radius, R_d, is compared with $R_{\rm ion}$ in Figure 1. At densities for which $R_d > R_{\rm ion}$, typically $n_{\rm H} \gtrsim 10^2\,{\rm cm}^{-3}$ (characteristic of star-forming regions), our neglect of absorption of $h\nu > 13.6\,$eV photons by dust in estimating $R_{\rm ion}$ is justified, because the dust will be destroyed by absorption of $h\nu < 7.5\,$eV photons prior to arrival of most of the ionizing photons at a given point in the cloud. At these densities, $h\nu > 13.6\,$eV photons are fully absorbed by the gas in a region smaller than the dust destruction zone, thus justifying our neglect of ionizing radiation when estimating R_d. Since the number of 7.5–13.6 eV photons is comparable to the number of $h\nu > 13.6\,$eV photons, this also shows that, for densities $n_{\rm H} \gtrsim 10^2\,{\rm cm}^{-3}$, the 7.5–13.6 eV photons will be mainly absorbed by H_2, and can be neglected for purposes of dust destruction.

At lower densities, where $R_d < R_{\rm ion}$, some fraction of $h\nu > 7.5$ eV radiation would also contribute to dust sublimation. At these densities the grain temperature near R_d is determined by radiative cooling and therefore $R_d \propto L^{1/2}$, where L is the UV luminosity available for dust heating. Since $L_{7.5-50} \simeq 2L_{1-7.5}$, the contribution of $h\nu > 7.5$ eV radiation may increase R_d by up to $\simeq 50\%$.

4. Electrostatic Disruption?

Because of the large fluence of energetic photons, dust destruction could, in principle, also result from extreme ionization of the dust grain. High degrees of ionization could result in fission

of the grain, or emission of individual ions from the grain surface by the process known as "ion field emission".

4.1. Coulomb Explosions?

For an approximately spherical grain of radius a, charged to a potential U, the tensile stress averaged over a cross section πa^2 is $S = (U/a)^2/4\pi$. If the maximum tensile stress which the grain material can support is $S_{\rm max}$, then the potential gradient and grain charge Z are limited by

$$\left(\frac{U}{a}\right) < 1.06 \times 10^8 \left(\frac{S_{\rm max}}{10^{10}{\rm dyne\,cm^{-2}}}\right)^{1/2} {\rm V\,cm^{-1}} \tag{21}$$

$$Z < 7.4 \times 10^4 \left(\frac{S_{\rm max}}{10^{10}{\rm dyne\,cm^{-2}}}\right)^{1/2} a_{-5}^2 \tag{22}$$

We note that if a grain with $S = S_{\rm max}$ fissioned into two halves, each of the fragments would have $S \approx 2^{-1/3} S_{\rm max}$ and there would therefore be no further fragmentation unless additional ionization took place.

A grain contains $\sim 3 \times 10^9 a_{-5}^3$ electrons. If the mean atomic number is ~ 10 and the photoionization cross section per electron is $\bar{\sigma} \approx 10^{-24}\,{\rm cm}^2$, then substantial grain destruction by this process would require a fluence $F(h\nu > 10{\rm keV}) \gtrsim 2.5 \times 10^{19} a_{-5}^{-1}\,{\rm cm}^{-2}$. Grain fission would therefore occur within a radius

$$R_{\rm Fis} \approx 30{\rm pc} E_{53}^{1/2} a_{-5}^{1/2} \tag{23}$$

where we have taken the fluence $F(h\nu > 10{\rm keV}) \approx (E/20{\rm keV})/4\pi R^2$. Note that this process changes the grain size distribution and therefore affects the optical extinction curve, but grain fission alone would not appreciably reduce the ultraviolet extinction, and might even increase it.

4.2. Ion field emission

Ideal materials have tensile strengths $S_{\rm max} \approx 10^{11}{\rm dyne\,cm^{-2}}$, so that a Coulomb explosion would not take place until the surface electric field reaches $U/a \approx 3 \times 10^8 {\rm V\,cm^{-1}}$. However, in the laboratory electric fields exceeding $\sim 3 \times 10^8 {\rm V\,cm^{-1}}$ are observed to result in "ion field emission", where individual ions are emitted from the sample (Muller & Tsong 1969). As a result, if the grain tensile strength $S_{\rm max} \gtrsim 10^{11}{\rm dyne\,cm^{-2}}$, intense irradiation by $h\nu \gtrsim 10{\rm keV}$ photons will first cause the grain to charge up to $Z_{\rm max} \approx 2.1 \times 10^5 (U/a)_{\rm max}$, and each subsequent ionization will result in emission of an ion (assuming that electron capture is negligible during the ~ 10 s of the gamma ray burst).

If the mean atomic number is ~ 10 and the photoionization cross section per electron is $\bar{\sigma} \approx 10^{-24}\,{\rm cm}^2$, then substantial grain destruction by this process would require a fluence

$F(h\nu > 10\mathrm{keV}) \gtrsim 10^{23}\,\mathrm{cm}^{-2}$. Grain destruction by ion field emission would therefore occur only within a radius

$$R_{\rm IFE} \approx 0.5 \mathrm{pc} E_{53}^{1/2} \tag{24}$$

Ion field emission is evidently much less important than sublimation.

5. Dust Infra-Red Emission

For clouds of mass $M < 10^7 M_\odot$ extending to $r \gtrsim 8$ pc, most of the optical-UV energy absorbed by sublimated dust is re-radiated in the infra-red, typically around $\lambda = 1\mu$m. This is due to the fact that at distances larger than $R_{\rm r=s} \approx 8L_{49}^{1/2}$ pc radiative cooling of dust grains dominates over sublimation cooling [see Eqs. (16,14)], and to the fact that for $M < 10^7 M_\odot$ grains are heated to the temperature $T_c \approx 2300$ K required for complete sublimation out to a distance $R_{\rm d} \approx 10$ pc [see Eq. (11), Fig. 1] (For $M > 10^7 M_\odot$, optical photons are completely absorbed at distances $\ll 10$ pc, where sublimation cooling dominates and only a small fraction of the absorbed energy is re-radiated).

At radii where radiation cooling dominates, the grain temperature drops approximately as $T \propto r^{-1/2}$. The strong dependence of grain survival time $t_{\rm surv}$ on temperature, Eq. (12), then implies a sharp transition, i.e. over a distance $\Delta r \ll R_{\rm d}$, between the region at $r < R_{\rm d}$ where $t_{\rm surv}$ is much smaller than the flash duration Δt, to the region at $r > R_{\rm d}$, where $t_{\rm surv} \gg \Delta t$. Since the energy radiated by grains is proportional to $\max(t_{\rm surv}, \Delta t)$, infra-red emission of sublimated dust is dominated by emission from grains just outside $R_{\rm d}$. If the optical depth for UV photons due to dust at $r > R_{\rm d} \approx 10$pc is $\tau_{\rm UV} \gtrsim 1$, then most of the flash energy would be absorbed by dust and re-radiated in the infra-red. Most of the infra-red radiation would escape the cloud, and may therefore be detected, if the infra-red optical depth is not high, $\tau_{\rm IR} \lesssim 1$. For $Q_{{\rm abs},\nu} \propto \nu^1$, the requirements $\tau_{\rm UV} \gtrsim 1$ and $\tau_{\rm IR} \lesssim 1$ may be written as $0.2 \lesssim \tau_V \lesssim 2$.

In order to estimate the dust infra-red luminosity in the case where $\tau_{\rm IR} \lesssim 1$ and $\tau_{\rm UV} \gtrsim 1$, let us first assume that optical-UV flash emission is beamed into a small solid angle around the line of sight, $\Delta\Omega = \pi\theta^2 \ll 4\pi$. The observed duration of the infra-red emission is then $\Delta t_{\rm IR} \approx R\theta^2/2c$, where $R \sim 10$ pc is the radius out to which grains are heated to ≈ 2300 K. This may be written in the form $\Delta t_{\rm IR} = 2(R/c)(\Delta\Omega/4\pi) \approx 20(\Delta\Omega/0.01)$ day, which is valid for $\Delta\Omega = 4\pi$ as well as for $\Delta\Omega \ll 4\pi$. The infra-red luminosity is given by the ratio of the flash energy absorbed by dust, $E_{1-7.5} \approx 10^{50}(\Delta\Omega/4\pi)$ erg, and the observed duration $\Delta t_{\rm IR}$, $L_{\rm IR} \approx E_{1-7.5}/\Delta t_{\rm IR} \approx 10^{41}$erg/s.

6. Implications

The luminosity of the prompt optical-UV emission accompanying GRB γ-ray emission is given by Eqs. (6) and (2). For typical GRB parameters we expect an optical-UV flash with

1–7.5 eV luminosity $L_{1-7.5} \approx 1 \times 10^{49}$erg/s, assuming isotropic emission. Such a UV flash can destroy dust by sublimation out to an appreciable distance, $R_{\rm d} \approx 10$ pc (see Figure 1), and may clear the dust out of $\sim 10^7(\Delta\Omega/4\pi)M_\odot$ of molecular cloud material, where $\Delta\Omega$ is the solid angle into which the optical-UV emission is beamed, and where dust is sublimed. If GRB sources indeed lie in dusty regions, then the extinction would decrease with time during prompt optical-UV emission, over tens of seconds. Detection of such time dependent extinction would provide strong constraints on the GRB environment. The destruction of dust implies that existing, or future, observations of not-heavily-reddened fireballs are not inconsistent with GRBs being associated with star formation.

We have shown in §5 that if the optical depth due to dust beyond ≈ 8 pc is of order unity, most of the UV flash energy is absorbed and re-radiated in the infra-red, typically at $\lambda \approx 1\mu$m. The resulting infra-red luminosity, $L_{\rm IR} \approx 10^{41}$erg/s, extends over an apparent duration of $\approx 20(1+z)(\Delta\Omega/0.01)$ day. For GRBs at $z = 1$, therefore, K-band photometry may reveal thermal emission from dust grains.

In fact, such emission may already have been observed in GRB970228 (Fruchter *et al.* 1999) and GRB980326 (Bloom *et al.* 1999). In both cases, a deviation from a power law decline of optical flux, which at early time is consistent with synchrotron emission from shock accelerated electrons, is observed at ~ 30 d delay. As the flux drops below $\sim 1\mu$Jy, a new infra-red emission component is revealed, with a flux $f_\nu \approx 0.5\mu$Jy between $\lambda = 2\mu$m and $\lambda = 1\mu$m for GRB970228 and $f_\nu \approx 0.7\mu$Jy at $\lambda = 0.9\mu$m for GRB980326. In both cases, the spectrum is modified at this time to $f_\nu \propto \lambda^3$ at $0.5\mu\text{m} \lesssim \lambda \lesssim 0.9\mu$m. The infra-red flux is of the same order of magnitude estimated for dust grain emission, and the spectrum is consistent with dust emission peaking at $\approx 1\mu$m (at the source redshift), provided GRB980326 is at redshift $z \sim 0.4$. We note that for the typical parameters adopted in this paper, dust emission is expected to peak at somewhat longer wavelength, $\approx 1.5\mu$m. However, since the grain properties are not well known, dust emission can not be ruled out as an alternative to the proposal that the "excess" emission is due to a supernova (Bloom *et al.* 1999, Reichart 1999, Galama *et al.* 1999) We note also that the non-detection of optical emission from GRB980326 at $t \sim 200$ d, implies, under the dust emission hypothesis, beaming of the optical-UV flash to $0.01 \lesssim \Delta\Omega \lesssim 0.1$, consistent with the interpretation that the rapid, t^{-2}, flux decline is due to the fireball being a jet of small opening angle (Rhoads 1999).

We have shown in §2 that strong optical-UV emission requires, like GRB γ-ray production, large initial expansion Lorentz factor, $\Gamma_i > 100$, which also implies that the plasma emitting the optical-UV flash must be expanding with $\Gamma > 100$. Thus, if the fireball is a jet of finite opening angle, $1 \gg \theta_j > 1/\Gamma \sim 0.01$, then both γ-ray and optical-UV emission will be confined to a small solid angle $\Delta\Omega = \pi\theta_j^2$. In this case, dust would be evaporated only within a narrow cone around the line of sight. A jet-like fireball expands as a conical section of a spherical fireball, with $\Gamma \propto t^{-3/8}$, as long as $\Gamma > 1/\theta_j$. After deceleration to $\Gamma < 1/\theta_j$, the jet expands sideways, its opening angle increasing to $\simeq 1/\Gamma$ and $\Gamma \propto t^{-1/2}$ (Rhoads 1999). At this stage radiation reaching us must travel a distance $l \approx r\sin(\Gamma^{-1} - \theta_j)/\sin(\theta_j)$ through gas which was not exposed to the

initial flash, and which will still contain dust. For $1 \ll \Gamma \ll 1/\theta_j$, and using $t \approx r/2\Gamma^2 c$, we have $l \approx r/\Gamma\theta_j \approx 2\Gamma ct/\theta_j \approx 0.1\mathrm{pc}(t/1\,\mathrm{week})^{1/2}/\theta_j^{2/3}$. Thus, a significant increase in extinction over time would be observed if $\theta_j \ll 0.1$.

Confinement of γ-ray and strong optical-UV emission to a small solid angle is not limited to the case of a jet-like fireball. It may also arise if Γ_i, the initial expansion Lorentz factor, is anisotropic. Consider a fireball carrying similar energy per unit solid angle in all directions, with Γ_i a decreasing function of angle with respect to the line of sight, such that $\Gamma_i \ll 300$ for $\theta > \theta_\gamma$. In this case, optical-UV (and γ-ray) emission would be suppressed at angles $\theta > \theta_\gamma$. The isotropic fireball energy per unit solid angle implies that, after a transition phase, the fireball would approach spherical expansion, with $\Gamma \propto t^{-3/8}$. At this stage, most of the radiation detected at time t by a distant observer is produced by fireball plasma within a narrow ring of radius $\simeq r/\Gamma$ around the line of sight, where the fireball radius r and expansion Lorentz factor $\Gamma(r)$ are related to t through $t = r/2\Gamma^2 c$ (Waxman 1997c). Thus, here too a significant increase in reddening is expected once Γ drops below $1/\theta_\gamma$. For $1 \ll \Gamma \ll 1/\theta_\gamma$ most of the radiation reaching us must pass through a path length $l \approx r/\Gamma\theta_\gamma \approx 2\Gamma ct/\theta_\gamma \approx 0.05\mathrm{pc}(t/1\,\mathrm{week})^{5/8}/\theta_\gamma$ of gas which was not exposed to the initial flash.

Finally, it should be noted that although optical flashes are expected for typical GRBs [with $E_{53} \approx 1$ and $n_0 \approx 1$, see Eq. (5)], prompt optical emission has been observed for only 1 GRB to date and therefore may not accompany all GRBs. Indeed, fireballs in low density environments with $n \ll 1\,\mathrm{cm}^{-3}$ would not be expected to produce strong prompt emission [see Eq. (5)]. In addition, if the fireball initial Lorentz factor $\Gamma_i \gg 300$, reverse shock emission may be shifted to photon energies above 7.5 eV [see Eq. (3)], where most photons are absorbed by H and H_2.

Acknowledgments. This work was supported in part by NSF grant AST-9619429. EW thanks the Institute for Advanced Study, Princeton for its hospitality during the period when this study was initiated.

REFERENCES

Akerlof, C. W., *et al.* 1999, GCN 205

Blandford, R. D., & McKee, C. F. 1976, Phys. Fluids 19, 1130

Bloom, J. S., *et al.* 1999, astro-ph/9905301

Böttcher, M. *et al.* 1998, astro-ph/9809156

Djorgovski, S. G., *et al.* 1999, GCN Circular No. 289

Draine, B.T. 1999a, http://www.astro.princeton.edu/~draine/dust/dust.diel.html

Draine, B.T. 1999b, submitted to ApJ (astro-ph/99997232)

Draine, B.T., & Lee, H.-M. 1984, ApJ, 285, 89

Fruchter, A. S., *et al.* 1999, ApJ, 516, 683

Galama, T. J., *et al.* 1999, astro-ph/9907264

Ghisellini, G. *et al.* 1998, astro-ph/9808156

Granot, J, Piran, T. & Sari, R. 1998, astro-ph/9808007

Gruzinov, A. & Waxman, E. 1999, Ap. J. 511, 852

Guhathakurta, P., & Draine, B.T. 1989, ApJ, 345, 230

Hogg, D. W. & Fruchter, A. S., submitted to Ap. J. (astro-ph/9807262).

Kouveliotu, C. *et al.* 1999, Nature, submitted

Krumholtz, M., Thorsett, S. E., & Harrison, F. A., Ap. J. **506**, L81 (1998).

Kulkarni, S. R., *et al.* 1998, Nature 395, 35

Loeb, A. & Perna, R. 1998, ApJ, 503, L35

Mau, S. & Mo, H. J. 1998, A&A 339, L1

Mészáros, P. & Rees, M. 1997, Ap. J. 476, 232

Mészáros, P. & Rees, M. 1999, submitted to MNRAS, (astro-ph/9902367)

Mészáros, P., Rees, M. & Papathanassiou, H. 1994, ApJ, 432, 181

Metzger, M. *et al.* 1997, IAUC 6676

Muller, E.W., & Tsong, T.T. 1969, Field Ion Microscopy (New York: American Elsevier)

Paczyński, B. 1998, Ap. J. 494, L45

Panaitescu, A. & Mészáros, P. 1998, ApJ, 501, 772

Park, H. S. *et al.* 1997, ApJ, 490, L21

Perna, R., & Loeb, A. 1998, ApJ, 501,467

Perna, R., Raymond, J., & Loeb, A. 1999, astro-ph/9904181

Piran, T. 1998, to appear in Phys. Reports (atro-ph/9810256)

Reichart, D. E. 1999, astro-ph/9906079

Rhoads, J. E. 1999, submitted to ApJ (astro-ph/9903399)

Sari, R., & Piran, T. 1999a, submitted to ApJ (astro-ph/9901338)

Sari, R., & Piran, T. 1999b, submitted to ApJ (astro-ph/9902009)

Waxman, E. 1997a, Ap. J. 485, L5

Waxman, E. 1997b, Ap. J. 489, L33

Waxman, E. 1997c, Ap. J. 491, L19

Wijers, R. A. M. J., & Galama, T. J. 1998, astro-ph/98050341

This preprint was prepared with the AAS LaTeX macros v4.0.

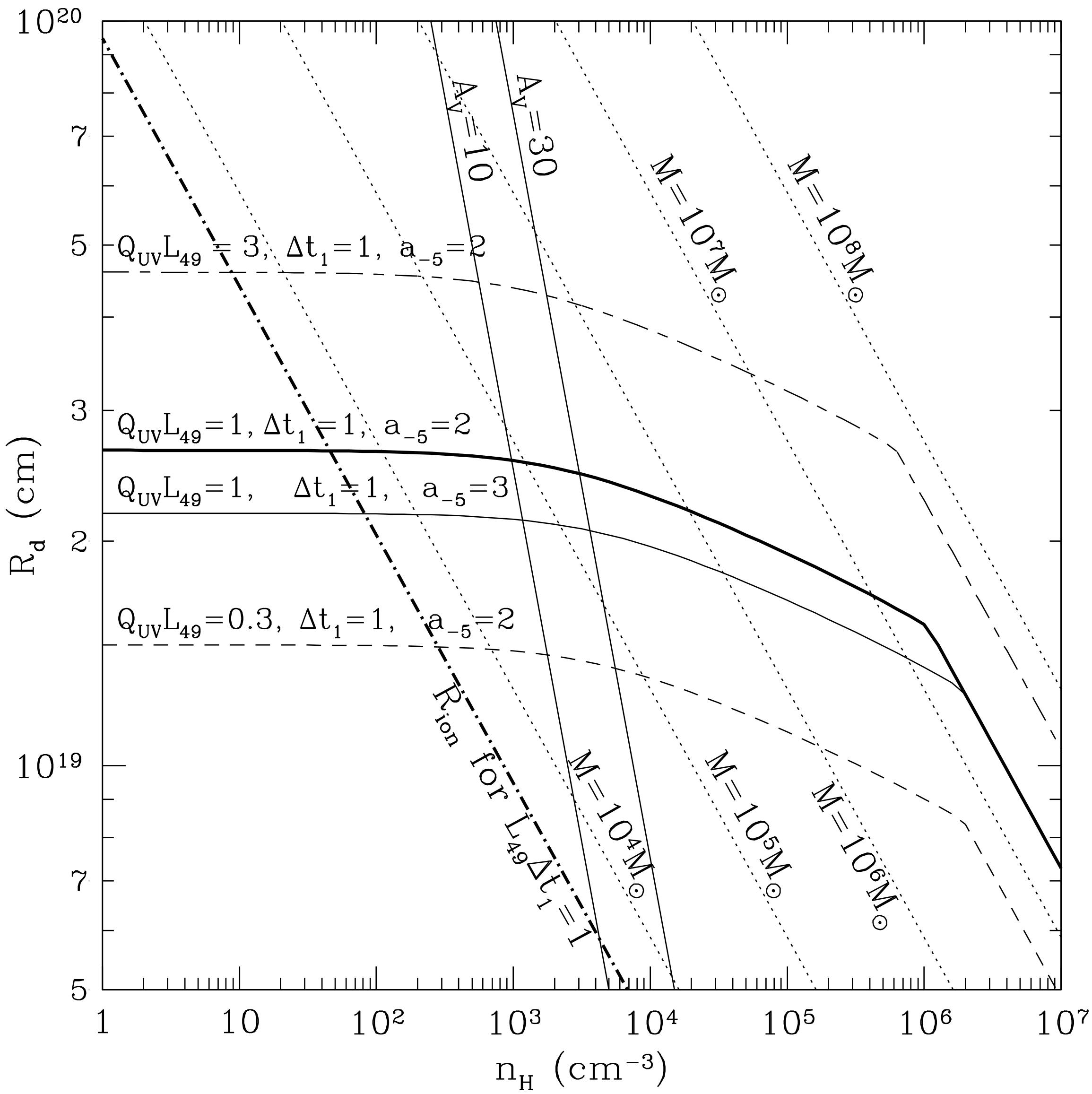

Fig. 1.— Radius $R_{\rm d}$ out to which grains are destroyed by thermal sublimation, as a function of cloud density $n_{\rm H}$, for different values of L_{49}, Δt_1, and a_{-5}. The heavy curve is for "typical" GRB parameters. The lines $A_V = 10$ and $A_V = 30$ show the radius of a cloud having $A_V = 10$ and 30 from center to edge. Also shown (broken line) is the radius $R_{\rm ion}$ out to which the gas is photoionized by a flash with $L_{49}\Delta t_1 = 1$. Dotted lines indicate radii with enclosed gas mass from $10^4 M_\odot$ to $10^8 M_\odot$.